Target-cell-specific facilitation and depression in neocortical circuits

Alex Reyes[1,2], R. Lujan[3,4], A. Rozov[1], N. Burnashev[1], P. Somogyi[3] and B. Sakmann[1]

[1] *Abteilung Zellphysiologie, Max-Planck-Institut für medizinische Forschung, Jahnstr. 29, D - 69120, Heidelberg, Germany*

[2] *Present address: Center for Neural Science, New York University, 4 Washington Place, New York, New York 10003-6621, USA*

[3] *Medical Research Council, Anatomical Neuropharmacology Unit, University Department of Pharmacology, Mansfield Road, Oxford, OX1 3TH, UK*

[4] *Present address: Instituto de Neurociencias, Universidad Miguel Hernandez, Facultad de Medicina, 03550 Alicante, Spain*

Correspondence should be addressed to B.S. (zpsecr@sunny.mpimf-heidelberg.mpg.de)

In neocortical circuits, repetitively active neurons evoke unitary postsynaptic potentials (PSPs) whose peak amplitudes either increase (facilitate) or decrease (depress) progressively. To examine the basis for these different synaptic responses, we made simultaneous recordings from three classes of neurons in cortical layer 2/3. We induced repetitive action potentials in pyramidal cells and recorded the evoked unitary excitatory (E)PSPs in two classes of GABAergic neurons. We observed facilitation of EPSPs in bitufted GABAergic interneurons, many of which expressed somatostatin immunoreactivity. EPSPs recorded from multipolar interneurons, however, showed depression. Some of these neurons were immunopositive for parvalbumin. Unitary inhibitory (I)PSPs evoked by repetitive stimulation of a bitufted neuron also showed a less pronounced but significant difference between the two target neurons. Facilitation and depression involve presynaptic mechanisms, and because a single neuron can express both behaviors simultaneously, we infer that local differences in the molecular structure of presynaptic nerve terminals are induced by retrograde signals from different classes of target neurons. Because bitufted and multipolar neurons both formed reciprocal inhibitory connections with pyramidal cells, the results imply that the balance of activation between two recurrent inhibitory pathways in the neocortex depends on the frequency of action potentials in pyramidal cells.

The efficacy of synaptic transmission in neuronal circuits is not constant but varies with the rate of action potentials in presynaptic neurons[1–5]. During a train of action potentials, the amplitudes of successively evoked postsynaptic potentials (PSPs) either increase (facilitate) or decrease (depress). An increase or decrease in the probability of transmitter release caused by the effects of successive action potentials in the presynaptic terminal are postulated to underlie short-term modification of PSPs[6–13]. One issue is the degree to which the identity of the presynaptic and the postsynaptic neuron determines facilitation or depression in a connection. In some synapses, the target cell is the primary determinant[14–25], whereas in others, it is the projecting neuron (refs 26, 27; A. Reyes & B.S., submitted). We recorded simultaneously from three neurons consisting of layer 2/3 pyramidal cells and two classes of interneurons in the neocortex of juvenile (postnatal day 14) rats and found that short-term modification of PSPs in identified interneurons is target-cell-specific but is mediated by presynaptic mechanisms. These studies represent one step in understanding organizing principles governing synaptic connections in the neocortex and may shed light on how neurons interact within a network.

Results

In neocortical brain slices visualized with infrared-differential contrast optics, three classes of neurons were selected based on their morphology (Fig. 1a) and their electrical excitability (Fig. 1b and c). Both multipolar and bitufted interneurons could, upon depolarizing current injection, discharge action potentials continuously at high rates (over 20 action potentials per second). Characteristically, however, the amplitude and frequency of action potentials decreased during a train in a class of bitufted neurons (Fig. 1b) but remained constant in multipolar cells (Fig. 1c). Pyramidal cells discharged at lower rates that decreased with time (not shown). A population of other interneurons was also identified, but they were not included in this study.

Pyramidal neurons formed excitatory connections with all three cell types. Suprathreshold intracellular stimulation of presynaptic pyramidal neurons evoked unitary excitatory (E)PSPs that were glutamatergic, as they were blocked by bath application of 30 μM CNQX and 50 μM APV (n = 14, data not shown). Nonpyramidal neurons also formed unitary connections with the three cell types. Postsynaptic potentials evoked by bitufted and multipolar neurons were completely and reversibly blocked by 20 μM bicuculline (n = 20, data not shown) and were classified as GABAergic inhibitory (I)PSPs. No evidence of nonGABAergic IPSPs was found. A further physiological criterion for classification of nonpyramidal cells was the frequency-dependent change in unitary EPSP amplitudes evoked by pyramidal cell stimulation. EPSPs facilitated in bitufted cells (Fig. 1b) but depressed in multipolar cells (Fig. 1c).

Identification of three classes of neurons was subsequently confirmed by reconstruction of the dendritic arbor of biocytin-labeled neurons. Pyramidal neurons had triangular somata with a prominent apical dendrite[28,29] that ended in a tuft in layer 1

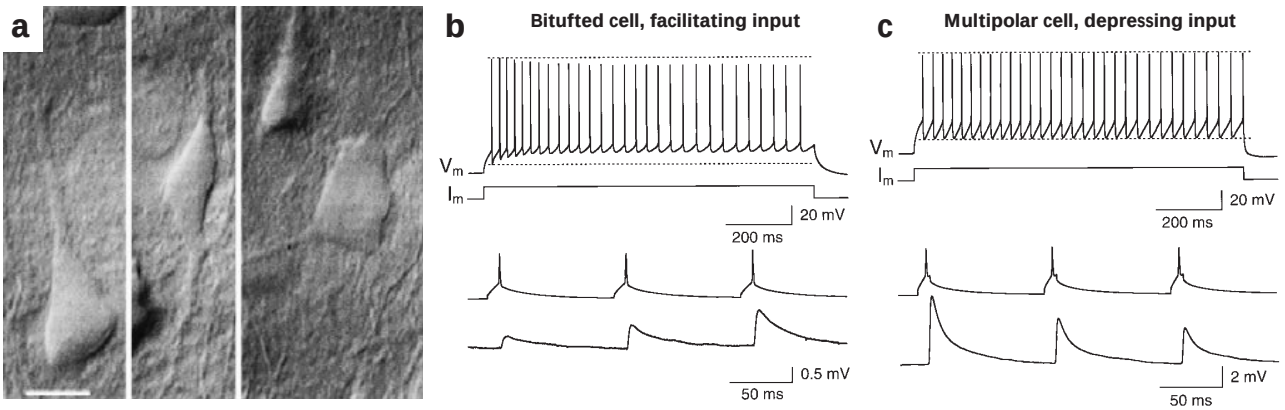

Fig. 1. Selection of three classes of neurons in layer 2/3. **(a)** Morphological selection. Representative infrared differential interference contrast enhanced video images of a pyramidal (left), bitufted (middle) and multipolar cell (right) in a slice of the somatosensory cortex taken from a two-week-old (P14) rat. These three classes were reliably identified in the living slice by the shape of their somata and by the location and number of proximal dendrites. Calibration bar is 10 µm and applies to all three images. **(b, c)** Functional selection. Upper pair of traces show action potential patterns of bitufted (b) and multipolar (c) neurons following injection of depolarizing current steps. The resting potentials were -68 mV and -70 mV. Lower pair of traces show the presynaptic action potentials and associated EPSPs evoked in bitufted and multipolar neurons during repetitive stimulation of the presynaptic pyramidal cell. The EPSPs evoked in the bitufted cell facilitated, whereas those evoked in the multipolar cell depressed. Amplitude calibrations refer to EPSPs. The EPSPs in this and subsequent figures are averages compiled from 50–200 sweeps and were evoked by delivering a 10 Hz train of brief current pulses to the presynaptic cells.

(Fig. 2a). Bitufted cells were characterized by ovoid somata from which one to four tufts of dendrites extended only in the apical and basal directions (Fig. 2a). Multipolar cells had round somata from which multiple dendrites extended radially (Fig. 2a).

Nonpyramidal cells have been grouped previously on the basis of connectivity and/or neurochemical markers[30,31]. To correlate these groups with the cell categories selected based on the microscope image, action-potential pattern and frequency-dependent, short-term modification of EPSPs, subsets of physiologically characterized neurons were immunolabeled for the neuropeptide somatostatin and the calcium-binding protein parvalbumin. Ten out of thirteen tested bitufted cells, with symmetrical dendritic arbors, were immunopositive for somatostatin (Fig. 2b), identifying them as a subset of GABAergic cells[32]. Eight somatostatin-positive cells were tested for synaptic modification; in all cases, the evoked EPSPs facilitated. None of five somatostatin-positive bitufted cells tested were immunoreactive for parvalbumin, although nearby cells displayed parvalbumin immunoreactivity. In contrast, all of the ten physiologically tested multipolar cells were immunonegative for somatostatin, but four of the five of

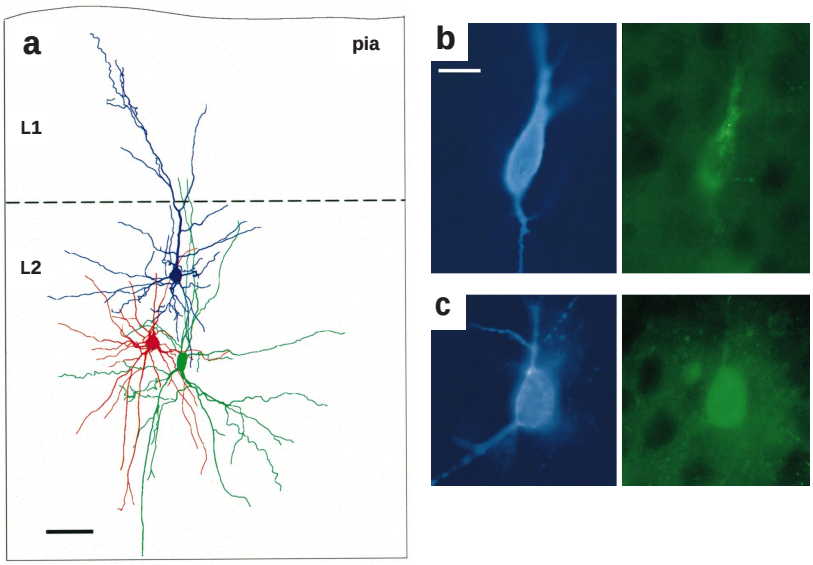

Fig. 2. Anatomical and immunocytochemical identification of layer 2/3 neurons. **(a)** Drawings of a pyramidal (blue), a multipolar (red) and a bitufted cell (green) labeled with biocytin (Methods) after simultaneous triple recording. Classification of the neurons was based on their discharge pattern and response properties of EPSPs to repetitive presynaptic action potentials. The axonal arbors are not shown for clarity. Calibration bar, 50 µm. Broken line indicates approximate border between cortical layer 1 (L1) and layer 2 (L2). The mean (± standard deviation) length, width and length per width of the somata for the cell types were, respectively, 17 ± 3 µm, 10 ± 2 µm and 1.7 ± 0.3 µm for pyramidal neurons (n = 23), 20 ± 3 µm, 8 ± 2 µm and 2.8 ± 1 µm (n = 20) for bitufted cells and 15 ± 3 µm, 11 ± 3 µm and 1.4 ± 0.3 µm for multipolar cells (n = 21) following fixation and dehydration. At the age range used, pyramidal and bitufted neurons were densely spiny, whereas multipolar cells were sparsely spiny. **(b)** Digital micrographs of a biocytin-labeled bitufted cell (left, visualized by AMCA-labeled streptavidin) that displayed electrophysiological characteristics typical of the population. The cell is immunopositive for somatostatin, as shown on the right by indirect FITC immunofluorescence. Calibration bar (10 µm) applies to both (b) and (c). **(c)** Digital micrographs of a biocytin-labeled multipolar cell (left, AMCA-labeled streptavidin) that displayed electrophysiological characteristics typical of the population. The cell is immunopositive for parvalbumin, as shown on the right by indirect FITC immunofluorescence.

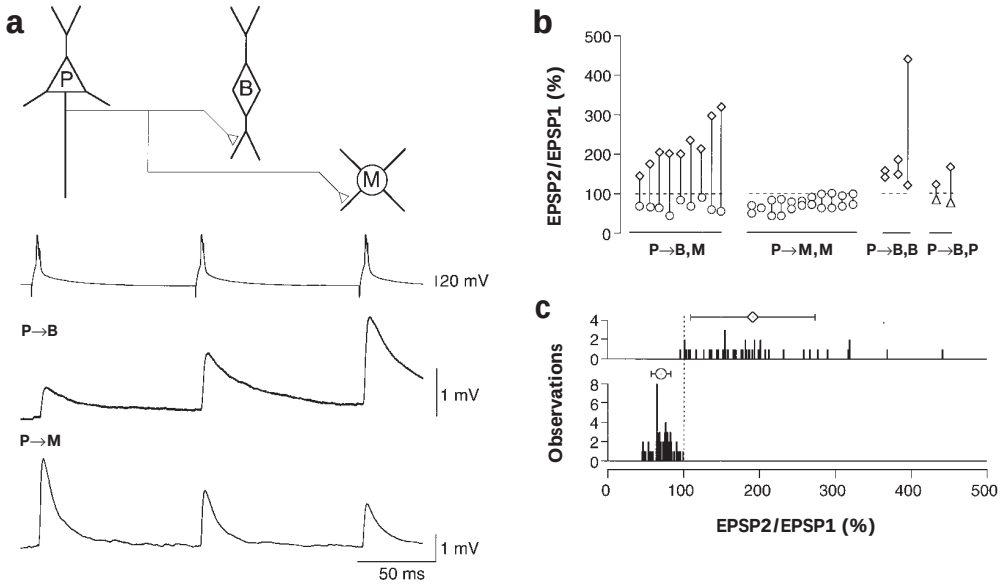

Fig. 3. Frequency-dependent, short-term modification of glutamatergic excitatory postsynaptic potentials evoked in two classes of neurons. **(a)** Simultaneous whole-cell recordings were made from a triplet (schematically shown on top) in which a pyramidal cell (P) innervated a bitufted (B) and a multipolar cell (M). When the pyramidal neuron was fired at 10 Hz (upper trace), the amplitude of the unitary EPSPs evoked successively in the bitufted cell increased (middle trace), whereas the amplitude of those evoked simultaneously in the multipolar cell decreased (lower trace). Resting potentials were -65 mV for the bitufted cell and -68 mV for the multipolar cell. **(b)** Pairwise comparison of short-term modification of EPSPs evoked in triple recordings. Each connected pair of symbols represents the amplitude ratio of EPSPs (amplitude of second EPSP to amplitude of first EPSP, in percent) evoked simultaneously in two target neurons during 10 Hz stimulation of the same presynaptic cell. The target neurons were either a bitufted and a multipolar cell (diamonds and circles); two multipolar cells (circles); two bitufted cells (diamonds); or a pyramidal and a bitufted cell (triangles and diamonds). **(c)** Distribution of amplitude ratios for EPSPs evoked in bitufted (upper histogram) and multipolar cells (lower histogram). Histograms include data from paired recordings. Symbols above histograms give the mean (± standard deviation) amplitude ratios. Means were 191 ± 82% for bitufted cells (n = 46, diamond) and 70 ± 13% for multipolar cells (n = 61, circle).

these tested were parvalbumin immunopositive (Fig. 2c), identifying them putatively as fast-discharging basket cells.

To assess how short-term modification of unitary EPSPs varied with the identity of target neurons, we recorded simultaneously from three cells where a single presynaptic neuron projected to two target neurons of different identity. In Fig. 3a, a pyramidal neuron innervated a bitufted and a multipolar neuron. Action potentials in the presynaptic pyramidal cell (at 10 Hz) evoked EPSPs that facilitated in the bitufted cell but simultaneously depressed in the multipolar cell. Facilitation and depression were maintained when the presynaptic neuron was stimulated at 20, 40 and 80 Hz (n = 6, data not shown). Figure 3b shows the amplitude ratios (amplitude of second EPSP to amplitude of first EPSP times 100, in percent) for EPSPs evoked simultaneously in bitufted and multipolar neurons. The amplitude ratios of EPSPs in bitufted cells were above 100%, whereas those of EPSPs in multipolar cells were all below 100% (significantly different, paired t-test, $p < 0.05$, n = 9 triple recordings). Target-cell-specific differences were also observed when one of the target neurons was pyramidal and the other bitufted (Fig. 3b). In addition, the amplitude ratios of EPSPs evoked in two multipolar target cells were both below 100%, whereas those of EPSPs evoked in two bitufted neurons were both above 100% (Fig. 3b). Figure 3c summarizes the distribution of EPSP amplitude ratios for EPSPs evoked in the two nonpyramidal target cells following stimulation of a pyramidal cell. For EPSPs evoked in bitufted cells, the mean (± standard deviation) amplitude ratio was 191 ± 82% (n = 46 connections), whereas that for EPSPs evoked in multipolar cells was 70 ± 13% (n = 61). The amplitude ratio of EPSPs evoked between pyramidal cells was 97 ± 23% (n = 44, data not shown; A.Reyes and B.S., submitted). The differences in the amplitude ratios were significant ($p < 0.05$; two-tailed t-test). Thus, frequency-dependent, short-term modification of unitary EPSPs evoked from axon collaterals originating from a single pyramidal cell varied with the identity of the target neuron, with the input to bitufted cells showing strong facilitation.

The target-specific differences in EPSP amplitude ratios were independent of the first EPSP of a train. Mean unitary EPSPs evoked by a single stimulus (at less than 0.2 Hz stimulation frequency) in multipolar cells (1.4 ± 1.4 mV; n = 61) were larger than those evoked in bitufted cells (0.25 ± 0.2 mV; n = 48). In bitufted cells, a linear regression fit to a plot of EPSP amplitude ratios versus EPSP amplitudes revealed no significant correlation; the slope was 145% per mV with r^2 = 0.18 (data not shown). For multipolar cells, the slope was -3% per mV (r^2 = 0.08). When comparison was limited to a small range of EPSP amplitudes (0.2–0.4 mV), the amplitude ratios for bitufted cells (177 ± 53%; n = 8) remained significantly ($p < 0.05$, two-tailed t-test) larger than those for the multipolar cells (77 ± 12%; n = 9).

Frequency-dependent facilitation of pyramid-to-bitufted cell connections implies that bitufted cells will be activated effectively by rapidly discharging pyramid cells. Bitufted cells are inhibitory and have as target neurons neighboring bitufted cells, multipolar cells and pyramidal cells. Synapses established by bitufted cells also showed short-term modification of IPSPs that depended on the identity of their targets. In Fig. 4a, a bitufted cell innervated both a bitufted and a multipolar cell. When the presynaptic bitufted cell was stimulated repetitively, the IPSPs evoked in the postsynaptic bitufted cell either exhibited small depression or facilitated weakly, while those evoked simultaneously in the multipolar cell depressed strongly. Figure 4b shows the amplitude ratios of IPSPs evoked simultaneously in a bitufted and either a

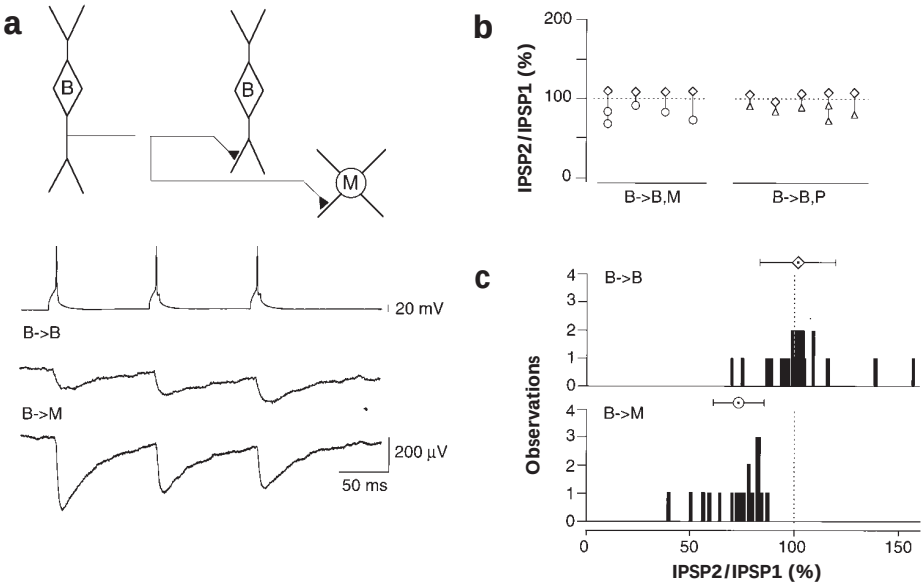

Fig. 4. Frequency-dependent short-term modification of GABAergic inhibitory postsynaptic potentials in two classes of interneurons. **(a)** Simultaneous whole-cell recordings were made from a triplet (shown on top), in which a bitufted cell (B) innervated another bitufted (B) and a multipolar (M) cell. The bitufted cell was stimulated at 10 Hz (upper trace). The associated IPSPs evoked in bitufted cells increased in amplitude (middle trace), whereas those evoked in the multipolar cell decreased (lower trace). **(b)** Pairwise comparison of short-term modification of IPSPs evoked in triplets. The connected symbols represent amplitude ratios of IPSPs evoked simultaneously in a bitufted (diamonds) and either a multipolar (circles) or a pyramidal (triangles) cell following 10 Hz stimulation of a presynaptic bitufted cell. **(c)** Distribution of amplitude ratios of IPSPs (IPSP2 to IPSP1, in percent) evoked by bitufted cell terminals in postsynaptic bitufted (upper histogram) and multipolar cells (lower histogram). Histograms include results from dual and triple recordings. Symbols above histograms give the mean (± standard deviation) IPSP amplitude ratios (bitufted cells, diamond, 101 ± 18%, n = 24; multipolar cells, circle, 73 ± 12%, n = 22).

multipolar or a pyramidal cell following stimulation of a presynaptic bitufted cell. Though facilitation of IPSPs, unlike the EPSPs, was not prominent in bitufted cells, the amplitude ratios of IPSPs evoked in bitufted cells were nevertheless significantly higher ($p < 0.05$; paired t-test; $n = 9$) than those evoked simultaneously in multipolar cells or pyramidal cells (Fig. 4b). The mean IPSP amplitude ratio, when the target neuron was a bitufted cell (Fig. 4c), was 101 ± 18 % ($n = 24$). This value was significantly ($p < 0.05$, two-tailed t-test) larger than that of IPSPs evoked in multipolar (73 ± 12%, $n = 22$; Fig. 4c) or in pyramidal cells (71 ± 15 %, $n = 22$; Fig. 6d).

To assess how transmitter release mechanisms contributed to facilitation or depression, we measured how frequently presynaptic action potentials failed to evoke an EPSP during a train of three stimuli. In a facilitating connection, the number of failures decreased progressively during the train, while the occurrence of large amplitude EPSPs increased. On average ($n = 20$ pairs), an increase in EPSP amplitude was accompanied by a decrease in the percentage of failures (Fig. 5a). In a depressing connection, the number of failures increased during the train while the EPSP amplitude decreased. The average ($n = 20$ pairs) decrease of EPSP amplitude was concomitant with an increase in the failure rate (Fig. 5c). The decrease in failure rate of the second EPSP was significant for facilitating connections (paired t-test; $p < 0.001$; mean difference, -14%; $n = 20$), as was the increase for depressing EPSPs ($p < 0.001$; mean difference, 15%; $n = 20$).

In facilitating connections, the increase in the mean amplitude of the second and third EPSP in the train was independent of the occurrence of the preceding EPSPs (Fig. 5b). In addition, the failure rate of the second EPSP was unaffected by the occurrence of the first EPSP ($p > 0.05$; paired t-test; $n = 15$). Thus, facilitation depended only on the occurrence of an action potential, regardless of whether it evoked an EPSP or not. In contrast, for the depressing connection, the amplitude of an EPSP in a train was larger when the preceding EPSPs failed to occur (Fig. 5d). Furthermore, the failure rate of the second EPSP increased significantly ($p < 0.02$; $n = 9$) by 9% when the first EPSP had occurred. These analyses indicate that a predominantly presynaptic mechanism underlies both facilitation and depression[6–25]. Facilitation, unlike depression, however, did not depend on release of transmitter from the presynaptic terminal, whereas depression required it.

A predominantly presynaptic mechanism for the frequency-dependent depression of IPSP amplitudes was further suggested by a coefficient of variation analysis of amplitude fluctuations of the first and second IPSPs in a train as determined for three connections. Plots (not shown) of the squared coefficients of variation against the mean peak amplitudes, both normalized to the respective control values, revealed that the data points were below the identity line[33].

Discussion

Target-cell-specific modification of PSPs has been reported in several excitatory[14–24] and inhibitory connections[25]. For excitatory projections to neocortical spiny stellate and pyramidal cells, synaptic modification depends primarily on the identity of the presynaptic neuron[27,34]. In the neocortical connections examined here, the postsynaptic bitufted cells determined facilitation of EPSPs and an increased paired-pulse ratio of IPSPs.

Several mechanisms can account for target specificity of release properties. A target neuron could locally modify release by transmitter-like substances that are liberated rapidly from the postsynaptic cell[35]. Because facilitation evoked by a train of action potentials is independent of a postsynaptic response (Fig. 5a and b), it is unlikely that modification of release by bitufted cells occurs on the time scale of the train. Depression, being dependent on release (Fig. 5c and d), could be generated by a rapid postsynaptic signal. On the other hand, the main difference between facilitating and depressing terminals could be a difference in the 'local-release fraction' of vesicles, i.e. the

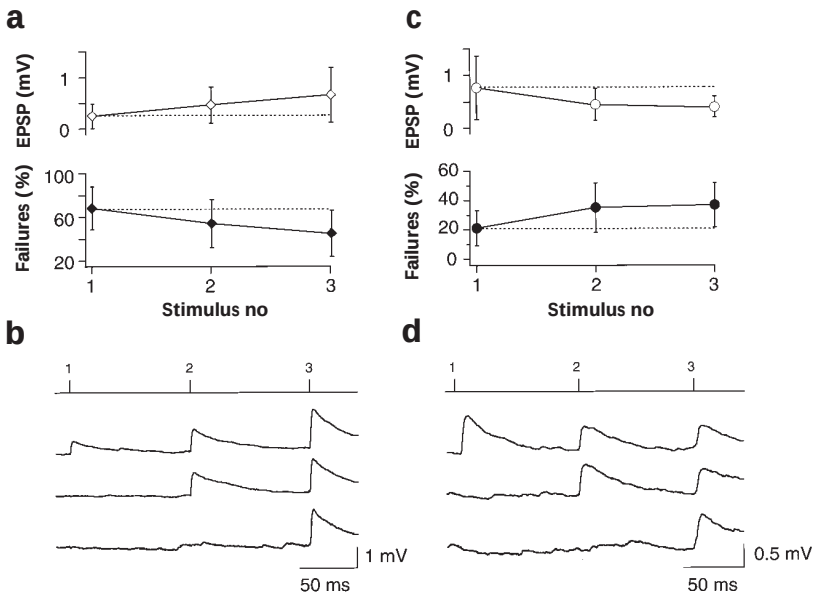

Fig. 5. Release mechanisms in presynaptic terminals underlie frequency-dependent short-term modification. **(a)** Mean (± standard deviation) percentage of failures (filled diamonds, lower graph) and mean amplitude (open diamonds, upper graph) of EPSPs evoked in bitufted cells during the first, second and third presynaptic action potentials (n = 20 connections). The number of failures decreased, whereas the EPSP amplitude increased. **(b)** Dependence of amplitudes of EPSPs evoked successively in a bitufted cell during suprathreshold stimulation of a presynaptic pyramidal cell. The time of occurrence of presynaptic action potentials is indicated schematically above voltage recordings. Numbers refer to the first, second and third action potential in a train. The average EPSPs evoked during first, second and third stimulus increased progressively (upper traces) from 0.7 mV to 1.1 mV and 1.9 mV, respectively. The middle trace shows the average EPSPs evoked by the second and third action potentials under the condition that the first action potential did not evoke an EPSP. The mean amplitudes of the EPSPs were 1.1 mV and 1.6 mV. The bottom trace shows an average of the third EPSP when the first and second action potentials failed to evoke EPSPs. The mean amplitude was 1.7 mV. The amplitude of the second EPSP was not significantly affected by the occurrence of the first EPSP ($p > 0.05$, paired t-test, $n = 15$). The amplitude of the third EPSP was similarly independent of the first and second EPSPs. **(c)** Plot of percentage of failures and mean amplitude of EPSPs evoked in multipolar cells during stimulation of presynaptic pyramidal neurons ($n = 20$). Only connections that exhibited failures to the first stimulus in the train were chosen for analysis. **(d)** Similar analysis for EPSP amplitudes as shown in (b) for a depressing connection between a pyramidal cell and a multipolar cell. The mean amplitudes for successive action potentials in the upper trace were 0.8, 0.5 and 0.5 mV. Those for the middle trace were 0.7 and 0.5 mV and that for the lower trace was 0.7 mV. The amplitude of the second EPSP was significantly ($p < 0.05$; paired t-test; $n = 9$) decreased by the occurrence of the first EPSP.

fraction of vesicles released by a single action potential. In facilitating terminals, this fraction would be small; in depressing terminals, it would be high. This local-release fraction depends on the structure of the release sites, including the density, subtype or state of calcium channels and the concentration and binding properties of endogenous calcium buffers. Therefore, factors from the postsynaptic cell, such as neurotrophins, which act on a much longer time scale[20], could modify locally the structure of presynaptic active zones.

Because pyramid-to-pyramid and pyramid-to-multipolar cell connections were different from pyramid-to-bitufted cell connections, and because both EPSPs and IPSPs show the same trend, one could argue the somatostatin-expressing bitufted neurons can influence, through a long-term mechanism, the structure of the active zone such that facilitation occurs. Somatostatin-containing bitufted neurons are unique in cortex also in that they express a very high level of the postsynaptic metabotropic glutamate receptor mGluR1a[36,37] and receive input from pyramidal cell recurrent axon terminals that have a very high level of the presynaptic metabotropic glutamate receptor mGluR7, located at the vesicle fusion site[36].

One functional consequence of the target-cell-specific facilitation and depression described here is that cortical excitation activates different local inhibitory pathways[30,31], depending on the rate of action potentials in pyramidal cells. Bitufted and multipolar cells are both connected reciprocally with pyramidal cells (Fig. 6a and b) via GABAergic inhibitory synapses. IPSPs in both connections showed the same degree of depression (Fig. 6c). Pyramidal neurons discharging at a low rate would preferentially excite multipolar inhibitory neurons, which will, via the feedback circuit, inhibit pyramidal cells. At higher rates, the facilitation of bitufted neuronal inputs would increasingly ensure recruitment of this population of neurons, which also inhibit pyramidal cells. One explanation of why these cells have pronounced frequency facilitation of their inputs may lie in their position in the cortical network. Their excitatory input could be dominated primarily by the level of local pyramidal cell activity, which is fed back to the distal dendrites of the pyramidal cells as GABAergic inhibition[30,31,38–40]. Thus, an increase in pyramidal-cell discharge frequency could shift the balance of GABAergic inhibition from a perisomatic location mediated by the parvalbumin-expressing multipolar cells to a dendritic location mediated by the somatostatin-expressing bitufted cells.

Methods

Brain slice preparation and visualization of neurons both in the living slice and after labeling with biocytin are described elsewhere[41,42]. During recordings, slices were maintained at 34^{0}C in extracellular solution consisting of (in mM) 125 NaCl, 2.5 KCl, 25 glucose, 25 H_2CO_3, 1.25 NaH_2PO_4, 2 $CaCl_2$ and 1 $MgCl_2$ (pH:7.2). Neurons were visualized via a 40x water immersion objective and two video cameras, which were mounted on a beam splitter so that the slice could also be viewed at two different magnifications (4x difference). Whole-cell voltage recordings were performed simultaneously from two or three neurons using pipettes with d.c. resistances of 5–15 MΩ when filled with (in mM) 100 K gluconate, 20 KCl, 4 ATP-Mg, 10 phosphocreatine, 0.3 GTP, and 10 HEPES (pH: 7.3; 310 mOsm). In synaptically connected neurons, suprathreshold intracellular stimulation of presynaptic cells evoked depolarizing EPSPs and IPSPs. In some experiments, intracellular solution contained

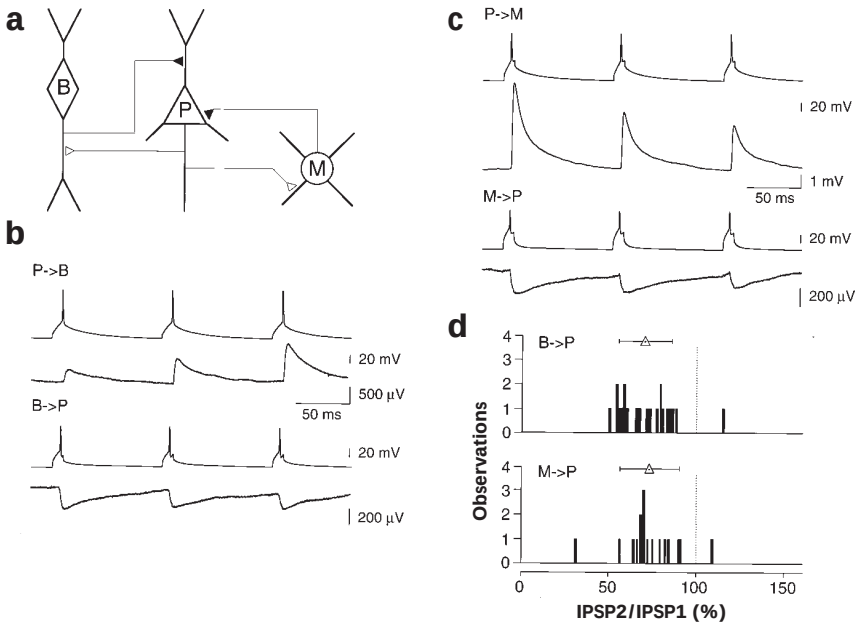

Fig. 6. Reciprocal excitatory and inhibitory connections between pyramidal and nonpyramidal cells. **(a)** Schematic diagram of reciprocal connections between a pyramidal cell, a bitufted cell and a multipolar cell in layer 2/3. **(b)** Dual recording from a pyramidal and a bitufted cell that were reciprocally connected. Both cells were stimulated alternately with trains of brief current pulses. (Action potentials are shown in first and third traces.) The EPSPs evoked in the bitufted cell facilitated (second trace), whereas the IPSPs evoked in the pyramidal cell depressed (fourth trace). **(c)** Dual recording from a pyramidal and a multipolar cell that were reciprocally connected. EPSPs evoked in the multipolar cell and IPSPs evoked in the pyramidal cell both depressed. Resting membrane potentials were -63 and -68 mV, respectively. **(d)** Summary of frequency-dependent depression of IPSPs in pyramidal cells evoked by 10 Hz stimulation of either bitufted or multipolar cells. Mean (± standard deviation) IPSP amplitude ratios were 71 ± 15% (n = 22) and 73 ± 17% (n = 17) for bitufted-to-pyramidal and multipolar-to-pyramidal cell connections, respectively.

4 mM KCl so that the IPSPs hyperpolarized. Both depolarizing and hyperpolarizing IPSPs were taken for analyses. Stimulus delivery, data acquisition and analyses were performed using macros in IGOR (Wavemetrics, Lake Oswego, OR). After data collection, whole-cell recording was re-established using pipettes filled with intracellular solution containing 0.5% biocytin. Morphological reconstruction of the labeled cells was subsequently performed using the Neurolucida tracing program (MicroBrightField, Colchester, VT).

Presynaptic cells were stimulated with a 10-Hz train of three to five suprathreshold current pulses. Trains were delivered at intervals of longer than 5 s, so that recovery from short-term modification was complete, as evidenced by the lack of systematic changes in the amplitude of the first PSP of a train during successive trains of stimuli. Voltage traces shown are averages of 50–200 sweeps.

The amplitude of the first EPSP of the train was defined as the difference between the peak of the EPSP and baseline. For the second or third EPSP, the amplitude was the difference between the peak of the EPSP and the baseline measured just before the peak onset. The time-to-peak of the EPSPs were sufficiently short so that temporal summation of the EPSPs did not introduce significant errors in the measurements of the peak amplitude. IPSPs had considerably longer time-to-peaks and decayed more slowly than EPSPs. To estimate the amplitude of the second IPSP, the decay of the first IPSP was fitted with a double exponential and extrapolated to the time corresponding to the peak of the IPSP. The IPSP amplitude was defined as the difference between the IPSP peak and the value of the extrapolated fit at the time of the peak.

For the neurochemical characterization of nonpyramidal cells, monoclonal antibodies to somatostatin (Code: SOMA8, recognizing somatostatin and SOM-28[43], ascites fluid diluted 1:500, visualized by fluorescein (FITC)-conjugated goat anti-mouse IgG, Jackson Lab) or monoclonal antibodies to parvalbumin (Sigma, No. P-3171, diluted 1:1000, visualized as above) were used sequentially on the same cell in an indirect immunofluorescence method. Each cell was examined after each layer of immunoreaction. The two antibodies gave nonoverlapping labeling patterns, and these served as controls for the method. The biocytin-filled cells were revealed by 7-amino-4-methylcoumarin-3-acetic acid (AMCA)-conjugated streptavidin (Vector Lab.). A Leica dichroic mirror system and the A4 filter block was used for recording AMCA, the L5 block for recording FITC fluorescence. Cells were recorded on a cooled CCD camera, analyzed and displayed using the Openlab software and color palette (Improvision, Coventry, UK). The immunonegativity of a cell for a marker could be due to damage caused by the recording, an undetectable low level of the molecule or the genuine absence of the marker. The consistent absence of parvalbumin from bitufted cells and somatostatin from multipolar cells strongly suggests the two cell populations are neurochemically different.

Following immunocytochemical characterization, the axonal and dendritic patterns of the cells were visualized by standard avidin-biotinylated-horseradish peroxidase complex (Vector Lab) and DAB reaction.

Acknowledgments

We thank E. Neher, B. Katz and G. Borst for their comments on the manuscript and B. Katz for suggesting the term 'local release fraction' of vesicles. We also thank J. C. Brown, at the MRC of Canada Group on Regulatory Peptides, Vancouver, for the gift of monoclonal antibodies to somatostatin, Z. Nusser and J. D. B. Roberts for assistance with digital micrography and Z. Ahmad for excellent technical assistance.

RECEIVED 24 APRIL; ACCEPTED 19 MAY 1998

1. Thomson, A. M., Deuchars, J. & West, D. C. Single axon excitatory postsynaptic potentials in neocortical interneurons exhibit pronounced paired pulse facilitation. *Neuroscience* 54, 347–360 (1993).
2. Thomson, A. M. & Deuchars, J. Synaptic interactions in neocortical local circuits: dual intracellular recordings *in vitro*. *Cereb. Cortex* 7, 510–522 (1997).
3. Markram, H. & Tsodyks, M. Redistribution of synaptic efficacy between neocortical pyramidal neurons. *Nature* 382, 807–810 (1996).
4. Thomson, A. M. Activity-dependent properties of synaptic transmission at two classes of connections made by rat neocortical pyramid axons *in vitro*. *J. Physiol. (Lond.)* 502, 131–147 (1997).
5. Buhl, E. H. *et al.* Effect, number and location of synapses made by single pyramidal cells onto aspiny interneurones of cat visual cortex. *J. Physiol. (Lond.)* 500, 689–713 (1997).

6. Del Castillo, J. & Katz, B. Statistical factors involved in neuromuscular facilitation and depression. *J. Physiol. (Lond.)* 124, 574–585 (1954).
7. Katz, B. & Miledi, R. The role of calcium in neuromuscular facilitation. *J. Physiol. (Lond.)* 195, 481–492 (1968).
8. Rahamimoff, R. A dual effect of calcium ions on neuromuscular facilitation. *J. Physiol. (Lond.)* 195, 471–480 (1968).
9. Betz, W.J. Depression of transmitter release at the neuromuscular junction of the frog. *J. Physiol. (Lond.)* 206, 629–644 (1970).
10. Zucker, R. S. Short-term synaptic plasticity. *Annu. Rev. Neurosci.* 12, 13–31 (1989).
11. Winslow, J. L, Duffy, S. N. & Charlton, M. P. Homosynaptic facilitation of transmitter release in crayfish is not affected by mobile calcium chelators: Implications for the residual ionized calcium hypothesis from electrophysiological and computational analyses. *J. Neurophysiol.* 72, 1769–1793 (1994).
12. Atluri, P. P. & Regehr, W. G. Determinants of the time course of facilitation at the granule cell to Purkinje cell synapses. *J. Neurosci.* 16, 5661–5671 (1996).
13. Zucker, R. S. Exocytosis: a molecular and physiological perspective. *Neuron* 17, 1049–1055 (1996).
14. Frank, E. Matching of facilitation at the neuromuscular junction of the lobster: a possible case for influence of muscle on nerve. *J. Physiol. (Lond.)* 233, 635–658 (1973).
15. Muller, K. J. & Nicholls, J. G. Different properties of synapses between a single sensory neuron and two different motor cells in the leech CNS. *J. Physiol. (Lond.)* 238, 357–369 (1974).
16. Koerber, H. R. & Mendell, L. M. Modulation of synaptic transmission at Ia-afferent fiber connections on motoneurons during high-frequency stimulation: Role of postsynaptic target. *J. Neurophysiol.* 65, 590–597 (1991).
17. Davis, G. W. & Murphey, R. K. A role for postsynaptic neurons in determining presynaptic release properties in the cricket CNS: Evidence for retrograde control of facilitation. *J. Neurosci.* 13, 3827–3838 (1993).
18. Katz, P. S., Kirk, M. D. & Govind, C. K. Facilitation and depression at different branches of the same motor axon: Evidence for presynaptic differences in release. *J. Neurosci.* 13, 3075–3089 (1993).
19. Brodin, L., Shupliakov, O., Pieribone, V. A., Hellgren, J. & Hill, R. H. The reticulospinal glutamate synapse in lamprey: Plasticity and presynaptic variability. *J. Neurophysiol.* 72, 592–604 (1994).
20. Davis, G. W. & Murphey, R. K. Long-term regulation of short-term transmitter release properties: retrograde signaling and synaptic development. *Trends Neurosci.* 17, 9–13 (1994).
21. Mennerick, S. & Zorumski, C. F. Paired-pulse modulation of fast excitatory synaptic currents in microcultures of rat hippocampal neurons. *J. Physiol. (Lond.)* 488, 85–101 (1995).
22. Ali, A. B. & Thomson, A. M. Brief train depression and facilitation at pyramid-interneurone connections in slices of rat hippocampus; paired recordings with biocytin filling. *J. Physiol. (Lond.)* 501, 9P (1997).
23. Ali, A. B. & Thomson, A. M. Facilitating pyramid to horizontal oriens-alveus interneurone inputs: dual intracellular recordings in slices of rat hippocampus. *J. Physiol. (Lond.)* 507, 185–199 (1998).
24. Ali, A. B., Deuchars J., Pawelzik H. & Thomson, A. M. CA1 pyramidal to basket and bistratified cell EPSPs: dual intracellular recordings in rat hippocampal slices. *J. Physiol. (Lond.)* 507, 201–217 (1998).
25. Atwood, H. L. & Bittner, G. D. Matching of excitatory and inhibitory inputs to crustacean muscle fibers. *J. Neurophysiol.* 34, 157–170 (1970).
26. Bower, J. M. & Haberly, L. B. Facilitating and nonfacilitating synapses on pyramidal cells: A correlation between physiology and morphology. *Proc. Natl. Acad. Sci. USA* 83, 1115–1119 (1986).
27. Stratford, K. J., Tarczy-Hornoch, K., Martin, K. A. C., Bannister, N. J. & Jack, J. J. B. Excitatory synaptic inputs to spiny stellate cells in cat visual cortex. *Nature* 382, 258–261 (1996).
28. Mason, A., Nicoll A. & Stratford, K. Synaptic transmission between individual pyramidal neurons of the rat visual cortex *in vitro*. *J. Neurosci.* 11, 72–84 (1991).
29. Schröder, R. & Luhmann, H. J. Morphology, electrophysiology and pathophysiology of supragranular neurons in rat primary somatosensory cortex. *Eur. J. Neurosci.* 9, 163–176 (1997).
30. Somogyi, P., Tamas, G., Lujan R. & Buhl, E. H. Salient features of synaptic organization in the cerebral cortex. *Brain Res. Rev.* 26, 113–135 (1998).
31. Kawaguchi, Y. & Kubota, Y. GABAergic cell subtypes and their synaptic connections in rat frontal cortex. *Cereb. Cortex*, 7, 476–486 (1997).
32. Somogyi, P. *et al.* Different populations of GABAergic neurons in the visual cortex and hippocampus of cat contain somatostatin- or cholecystokinin-immunoreactive material. *J. Neurosci.* 4, 2590–2603 (1984).
33. Faber, D. S. & Korn, H. Applicability of the coefficient of variation method for analyzing synaptic plasticity. *Biophys. J.* 60, 1288–1294 (1991).
34. Gil, Z., Connors I. W. & Amitai, Y. Differential regulation of neocortical synapses by neuromodulators and activity. *Neuron* 19, 679–686 (1997).
35. Glitsch M., Llano I. & Marty, A. Glutamate as a candidate retrograde messenger at interneurone-Purkinje cell synapses of rat cerebellum. *J. Physiol. (Lond.)* 497, 531–537 (1996).
36. Shigemoto, R. *et al.* Target-cell-specific concentration of a metabotropic glutamate receptor in the presynaptic active zone. *Nature* 381, 523–525 (1996).
37. Baude, A. *et al.* The metabotropic glutamate receptor (mGluR1α) is concentrated at perisynaptic membrane of neuronal subpopulations as detected by immunogold reaction. *Neuron* 11, 771–787 (1993).
38. Blasco-Ibanez, J. M. & Freund, T. F. Synaptic input of horizontal interneurons in stratum oriens of the hippocampal CA1 subfield: Structural basis of feed-back activation. *Eur. J. Neurosci.* 7, 2170–2180 (1995).
39. Han, Z.-H., Buhl, E. H., Lörinczi Z. & Somogyi, P. A high degree of spatial selectivity in the axonal and dendritic domains of physiologically identified local-circuit neurons in the dentate gyrus of the rat hippocampus. *Eur. J. Neurosci.* 5, 395–410 (1993).
40. Maccaferri, G. & McBain, C. J. Passive propagation of LTD to stratum oriens-alveus inhibitory neurons modulates the temporoammonic input to the hippocampal CA1 region. *Neuron* 15, 137–145 (1995).
41. Stuart, G. J., Dodt, H. U. & Sakmann, B. Patch clamp recordings from the soma and dendrites of neurones in brain slices using infrared video microscopy. *Pflügers Arch.* 423, 511–518 (1993).
42. Markram, H., Lübke, J., Frotscher, M., Roth, A. & Sakmann, B. Physiology and anatomy of synaptic connections between thick tufted pyramidal neurones in the developing rat neocortex. *J. Physiol. (Lond.)* 500, 409–440 (1997).
43. Vincent S. R., McIntosh, C. H., Buchan, A. M. & Brown, J. C. Central somatostatin systems revealed with monoclonal antibodies. *J. Comp. Neurol.* 238, 169–186 (1985).